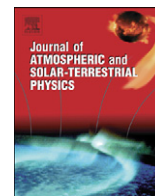




ELSEVIER

Contents lists available at SciVerse ScienceDirect

Journal of Atmospheric and Solar-Terrestrial Physics

journal homepage: www.elsevier.com/locate/jastp

Ion-neutral coupling during deep solar minimum

Cheryl Y. Huang^{a,*}, Patrick A. Roddy^a, Eric K. Sutton^a, Russell Stoneback^b, Robert F. Pfaff^c, Louise C. Gentile^a, Susan H. Delay^d^a Air Force Research Laboratory, Space Vehicles Directorate, Kirtland AFB, NM, USA^b William B. Hanson Center for Space Sciences, University of Texas at Dallas, Richardson, TX, USA^c NASA/Goddard Space Flight Center, Greenbelt, MD, USA^d Institute for Scientific Research, Boston College, Chestnut Hill, MA, USA

ARTICLE INFO

Article history:

Received 2 August 2012

Received in revised form

18 October 2012

Accepted 16 November 2012

Keywords:

Equatorial ionosphere

Thermosphere

Nonmigrating tides

Plasma depletions

ABSTRACT

The equatorial ionosphere under conditions of deep solar minimum exhibits structuring due to tidal forces. Data from instruments carried by the Communication/Navigation Outage Forecasting System (C/NOFS) which was launched in April 2008 have been analyzed for the first 2 years following launch. The Planar Langmuir Probe (PLP), Ion Velocity Meter (IVM) and Vector Electric Field Investigation (VEFI) all detect periodic structures during the 2008–2010 period which appear to be tides. However when the tidal features detected by these instruments are compared, there are distinctive and significant differences between the observations. Tides in neutral densities measured by the Gravity Recovery and Climate Experiment (GRACE) satellite were also observed during June 2008. In addition, Broad Plasma Decreases (BPDs) appear as a deep absolute minimum in the plasma and neutral density tidal pattern. These are co-located with regions of large downward-directed ion meridional velocities and minima in the zonal drifts, all on the nightside. The region in which BPDs occur coincides with a peak in occurrence rate of dawn depletions in plasma density observed on the Defense Meteorological Satellite Program (DMSP) spacecraft, as well as a minimum in radiance detected by UV imagers on the Thermosphere Ionosphere Mesosphere Energetics and Dynamics (TIMED) and IMAGE satellites.

Published by Elsevier Ltd.

1. Introduction

During the recent deep solar minimum, the equatorial ionosphere has exhibited behavior which was quite unexpected. A description of the differences in ionospheric structure observed during deep solar minimum is given by Heelis et al. (2009). Most studies of the ionosphere prior to the launch of the C/NOFS mission have focused on external forcing by magnetic activity such as storms in which energy from the solar wind is imposed on the ionosphere–thermosphere (IT) system leading to dramatic variations in plasma densities and velocities at all latitudes. However during deep solar minimum when external forces were largely absent, internal forcing from the lower atmosphere became dominant. The surprising result was that lower atmosphere forcing caused changes in ionospheric structure which are persistent up to altitudes of 800 km and above. This paper focuses on IT coupling during the 2008–2010 period when forcing from below was the main contributor to ionospheric structure. While tidal features have been observed during all phases of the solar cycle (Scherliess et al., 2008), during the recent solar minimum

the entire ionosphere is structured by tidal forcing as we will show below. As a result, tidal signatures are readily apparent in many independent observations although with significant differences between the different datasets.

Extensive studies of plasma irregularities have established the complex relationship between E- and F-regions' electric fields and neutral winds driving the growth of the Rayleigh–Taylor instability (see de La Beaujardière et al., 2004 and references therein). The C/NOFS satellite was launched in April 2008 with the aim of predicting communication outages due to these equatorial irregularity structures. To the surprise of many, C/NOFS observations of large-scale ionospheric structuring dominated observations during the period following launch.

Recent studies have indicated the importance of the troposphere as a major contributor to ionospheric structure. Migrating and nonmigrating tides (Lindzen and Chapman, 1969) are generated by an interaction between tropospheric latent heat and solar diurnal tides which are generated by solar radiation (Hagan and Forbes, 2002, 2003). Discovery that these tides penetrate deep into the upper F-region up to altitudes above 800 km was surprising, as planetary waves are expected to damp out far below the F-region peak. Results from the C/NOFS mission have confirmed that tidal structures are dominant in the ionosphere, with reports from a number of separate investigations over the entire altitude range of

* Corresponding author. Tel.: +1 505 846 7218; fax: +1 505 853 7822.

E-mail address: cheryl.huang@us.af.mil (C.Y. Huang).

the satellite (Araujo-Pradere et al., 2012; Dao et al., 2011; Pfaff et al., 2010a). In this paper we present an analysis of longitudinal structures found in C/NOFS plasma densities and velocities, and focus on one particular phenomenon called a Broad Plasma Decrease (BPD), first reported by Huang et al. (2009).

In our first paper on BPDs (Huang et al., 2009), we pointed out that they appeared on C/NOFS, the DMSP satellite, and the Challenging Minisatellite Payload (CHAMP) as large decreases in plasma and neutral density, as well as plasma temperature, extending across hours of local time in longitude, and up to 30° in latitude. They were observed persistently during solar minimum periods on DMSP in the 20–22 LT sector, and almost every day on C/NOFS during June 2008. Their preferred location is around 300° – 360° longitude, although they are also observed at other longitudes.

In subsequent studies (Huang et al., 2011, in press), using altitude-detrended PLP data, we established that BPDs are part of a pattern of wavenumber-4 periodicity in which they form a very deep minimum persistently around 330° longitude. Neutral density residuals from the GRACE satellite also exhibit 4-wave periodicity, and a similar deep decrease in density is observed in the same location at BPDs. 4-Wave signatures were also found in averaged IVM data, with large negative velocities detected in the vicinity of the BPDs. The climatology of the periodic signatures in PLP data was shown to be approximately that of the Diurnal Eastward-propagating nonmigrating tide of wavenumber 3 (DE3) which appears as a 4-wave longitudinal structure in an inertial frame.

Similar structures have been reported by many investigators in the DMSP plasma data (Ren et al., 2008; Huang et al., 2010), CHAMP electron densities (Lühr et al., 2007; Liu and Watanabe, 2008; Pedatella et al., 2008), vertical plasma drifts on ROCSAT and C/NOFS (Kil et al., 2007; Araujo-Pradere et al., 2012) and Total Electron Content (TEC) (Lin et al., 2007; Scherliess et al., 2008; Pancheva and Mukhtarov, 2010) and others. Longitudinal structuring appears in Far UltraViolet (FUV) observations from IMAGE, and the Global UltraViolet Imager (GUVI) measurements on the TIMED satellites (Immel et al., 2006), where peak radiance in the equatorial arcs can be directly related to plasma density. The Global Scale Wave Model (GSWM) (Hagan et al., 2001; Hagan and Forbes, 2002, 2003) predictions of wave formation agree well with the FUV observations.

It should be noted that the PLP tidal signatures occur in the total densities, not in a residual analysis. This distinguishes our observations from most past investigations of this phenomenon. During the 2008–2010 interval, the entire ionosphere is dominated by tidal forcing which imposes variations in in situ density up to 35% on the dayside. This exceeds the variation of 20% reported in past investigations of tides in total electron content (Scherliess et al., 2008). In addition we compare the tidal structures in plasma density with those in ion drift and electric fields observed from the same spacecraft, and discuss the similarities and differences between the observations.

In the following sections of this paper, we present simultaneous observations made by instruments on the C/NOFS, DMSP and GRACE spacecraft. These observations are of plasma density, velocity and electric fields from C/NOFS, plasma density from DMSP and neutral density from GRACE. We discuss how these correlated results compare, where they differ, and their significance for an understanding of ionospheric structure. Finally, we return to the BPDs, comparing them with similar phenomena reported previously and suggest how they relate to tidal structure.

2. Instrumentation

The C/NOFS satellite was launched in April 2008 into a low inclination (13°) elliptical ($401 \times 850 \text{ km}^2$ altitude) orbit, with an

orbital period of 97.3 min. The PLP on C/NOFS measures plasma densities, electron temperatures and density fluctuations at rates ranging from 32 to 1024 samples per second. We have used 1-min averaged plasma density data for our analysis. During the period of this study, large density depletions were observed over the full altitude range of the C/NOFS orbit.

The IVM on C/NOFS records three-dimensional ion velocities, densities and temperatures in 0.5 s. For this study, we restricted our analysis to meridional velocities, velocities in the coordinate system defined by the Earth's magnetic field. In this frame of reference, velocity in the horizontal plane is meridional (directed along a line of longitude) or zonal (directed along a line of latitude). Positive values of the meridional velocity indicate ion velocity along the meridian directed away from the Earth while negative values indicate ion velocity toward the Earth. All velocities were projected to the equator assuming that dipole magnetic field lines are equipotentials, and that the electric field at the equator can be related to the electric field at a location off the equator by the relative magnetic field strengths. Due to the low ambient plasma densities, the results in this study were restricted to periods when the satellite was below 500 km during 2009 and O^+ densities above threshold for the instrument. To obtain full coverage of all local times at these altitudes, we show 3-month averages in this paper.

Vector measurements of the DC electric field on the C/NOFS satellite are provided by the Vector Electric Field Investigation (VEFI) which includes a 3-axis detector that gathers DC and AC (or wave) electric fields using the double probe technique (e.g., Maynard, 1998). As described in Pfaff et al. (2010b), the VEFI instrument includes six rigid 9.5 m booms that extend 11.8 cm diameter spherical sensors with embedded pre-amplifiers. The booms are oriented to provide three orthogonal 20 m tip-to-tip double probes that detect three components of the vector DC and AC electric fields. DC electric fields are sampled at 2048 times per second by digitizing the potential differences between opposing sensors using 16-bit A/D converters. The standard DC electric field waveforms are subsequently filtered and averaged on-board the satellite to produce three 16 sample/s components prior to telemetry to the ground. Advanced processing techniques are used to identify and subtract contact potentials, offsets, and sheath-related electric fields in order to assure high quantitative accuracy (Pfaff et al., 2010b).

In this paper we use only the zonal drifts obtained from the cross product of the meridional electric field component and the Earth's magnetic field given by the International Reference Geomagnetic Field (IGRF) model. Structured fields within active irregularities are rejected if the rms error in the preceding 10 s is greater than 30 m/s (John Retterer, private communication, 2012). Electric field values were projected to the equator using IGRF, as was done for the IVM meridional velocities. The data have been averaged into 120-day bins for the solstices, and 60-day bins for equinoxes. The width of the longitudinal bins is 15° .

Neutral densities on the GRACE satellite were measured using superSTAR accelerometers, using the techniques of Sutton et al. (2005) and Sutton (2009). These measurements are similar to those made by the STAR accelerometer on CHAMP (Bruinsma et al., 2004; Sutton, 2009), with a precision an order of magnitude greater than the CHAMP instrument. In this study, 5-second data were used. During the period of interest, the satellite is in a $443 \times 485 \text{ km}^2$ orbit. Factoring in the oblateness of the Earth, the minimum altitude in the World Geodetic System 84 (WGS84) was 460 km and the maximum was 506 km.

GRACE makes 30–32 equatorial passes per day; 15–16 on the ascending portion of its orbit and 15–16 on the descending. Given the rotation of the Earth, each of the passes occurs over a different longitude such that after a day, there are 15–16 data points

equally spaced in longitude, per hemisphere. The repeat ground-track period is 7 days, after which time there are about 112 data points equally spaced in longitude, per hemisphere. The GRACE plots in this paper use 28 days, so there are 4 repeat ground tracks in longitude, with limited coverage of local times. In this paper we include only those local times for which we have sufficient numbers of observations. We restrict the data to the same latitude range as that covered by the C/NOFS satellite during June 2008.

DMSF spacecraft fly in Sun-synchronous, 98.7°-inclined circular orbits at altitudes near 840 km. F17 was launched in November 2006. During the years of interest the descending node was near the 0530 LT meridian. On average each spacecraft completes 14 orbits per day or ~ 5100 orbits per year. From one orbit to the next the descending node advances in longitude by $\sim 25^\circ$. Plasma density depletions were measured by an ion trap that faces in the ram direction (Rich and Hairston, 1994).

3. Observations

In this paper, we use altitude-detrended PLP data. The methodology was described by Huang et al. (2011, 2012). To summarize briefly, we remove the effects of spacecraft altitude and its effect on plasma density by scaling the measured density to a common location at 500 km and a common latitude at 0° . To do this, we use the 2007 version of the International Reference Ionosphere (Bilitza and Reinisch, 2008) model. We take the location of the C/NOFS satellite at each point along the orbit, determine the IRI value of the plasma density at that location (same universal time, longitude, latitude, altitude, solar F10.7 index) and the IRI density at 500 km at the equator for the same universal time, longitude, and F10.7 index. The ratio of IRI (C/NOFS location)/IRI (500 km, 0°) gives us the scaling factor which we use to detrend all the PLP data used in this and previous studies.

Fig. 1 shows the effect of altitude detrending on the PLP data. On the left are shown the PLP measurements of plasma density on 19 June 2008, orbit 953, from 22:09 to 23:33 UT. At right are shown the detrended data for this orbit. The PLP measurements are plotted in blue, the IRI predictions are shown in red. There are clear differences between IRI and the PLP measurements in both plots, with lower densities being observed than models predict. As the recent solar minimum was the lowest recorded solar activity since the start of the space age, this was to be expected.

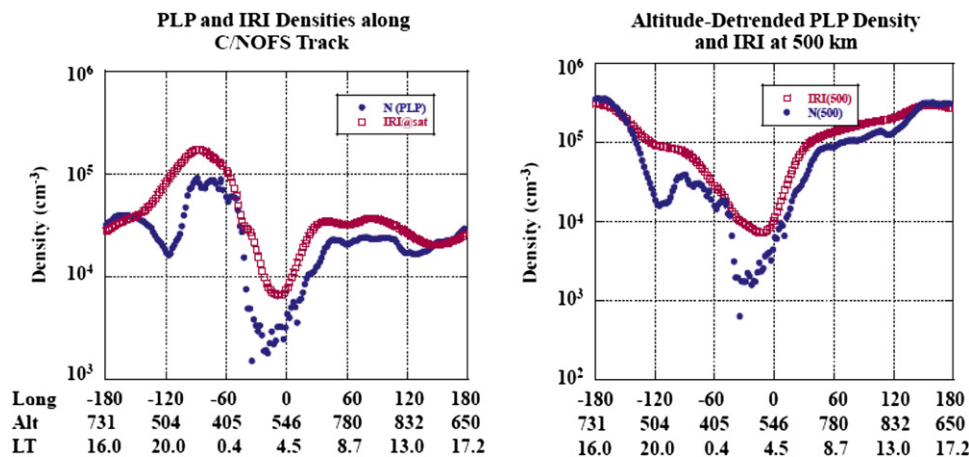


Fig. 1. PLP data for orbit 953 on 19 June 2008. The time interval spans 2209–2333 UT. On the left are shown the original data (blue) with the IRI model prediction (red). On the right are shown the detrended PLP data (blue) projected to an altitude of 500 km at the equator. IRI model values for the projected PLP locations are shown in red. (For interpretation of the references to color in this figure legend, the reader is referred to the web version of this article.)

The differences between the initial and altitude-detrended PLP data are also clear. The range of values expanded with both higher and lower values in the detrended data. Note that our detrending scheme has not removed all orbital effects. When plotted for an extended period, there are still small variations which appear to be related to the precession rate. However the features we discuss in this paper are much larger than these small oscillations.

Fig. 2 shows the results of the altitude detrending and averaging of the PLP plasma densities. Four month-long periods have been chosen as representatives of the seasons during 1 year. There are clear periodic structures apparent, most clearly in March, June and September, and strongest on the dayside. These exhibit wavenumber-4 periodicity. Wavenumber-4 signatures are a persistent feature in many of the instrument results on C/NOFS during the 2008–2010 period (Dao et al., 2011; Araujo-Pradere et al., 2012 and others).

In addition to the 4-wave periodicity which is strongest on the dayside, there is also a persistent deep minimum in plasma density most evident on the nightside, between 300° and 360° . We have described these as Broad Plasma Decreases (BPDs) previously (Huang et al., 2009, 2011, 2012).

Fig. 3 shows the IVM meridional velocities for the 3-month interval August–October in 2009 (top) and 2010 (bottom). The 4-peaked structure can be seen, most strongly on the dayside. Note the negative meridional velocities on the nightside peaking at a maximum of -45 m/s at approximately 60° and 330° longitude, coincident with the occurrences of BPDs.

Fig. 4 shows the zonal drifts from VEFI during three northern summer solstices in 2008–2010. The strongest wavenumber-4 signatures occurred during 2008 when solar activity reached a minimum, but periodicity is also apparent in 2009 and 2010. As with PLP and IVM, the strongest wave periodicity occurs on the dayside, peaking around 12 LT.

Note that there are wavenumber-4 features in the VEFI zonal drifts on the nightside during 2008 and 2009 between 18 and 22 LT. During 2010 there are also wavenumber-4 structures at these local times, but they are less distinct than in the two previous summer intervals. These nightside wave structures are not apparent in other C/NOFS instruments. Between the post-sunset and post-midnight local times, there appears to be a phase shift in the VEFI structures, shown in Fig. 5 in which the zonal drifts at 3.25 and 21.75 LT are shown for the same three seasons as in Fig. 4. The main differences occur between 180° and 360° . Where the drift at 21.75 LT shows a weak maximum around 180° , there is a minimum at 3.25 LT. However the biggest differences occur

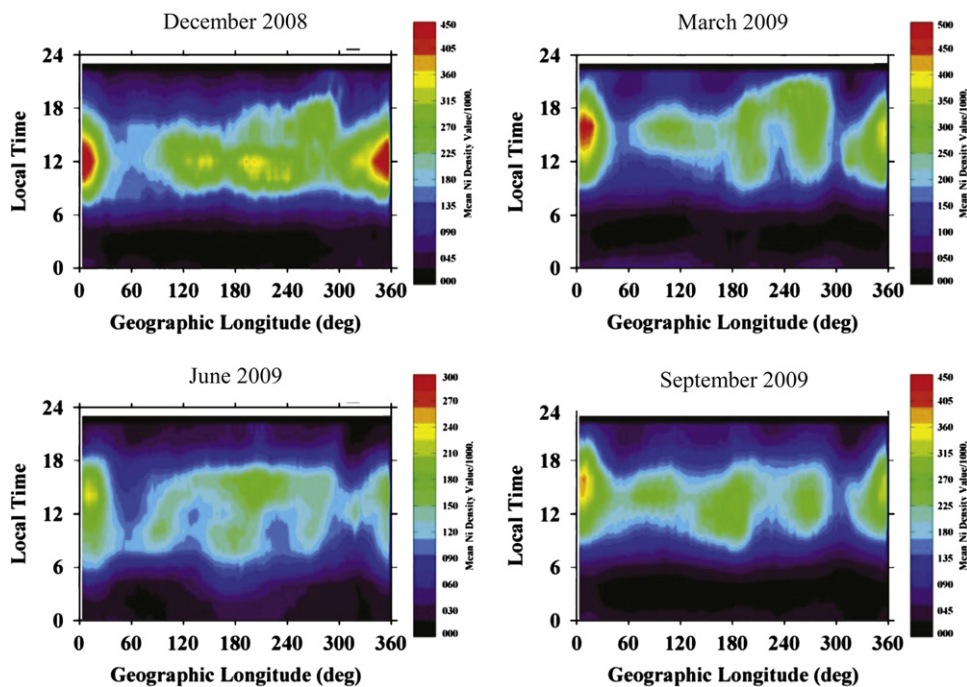


Fig. 2. Results for the averaged detrended PLP data are shown for four representative months. From top-left, is shown the data for December 2008. At top-right, are shown the data for March 2009. At bottom-left, are shown the data for June 2009. At bottom-right, are shown the data for September 2009.

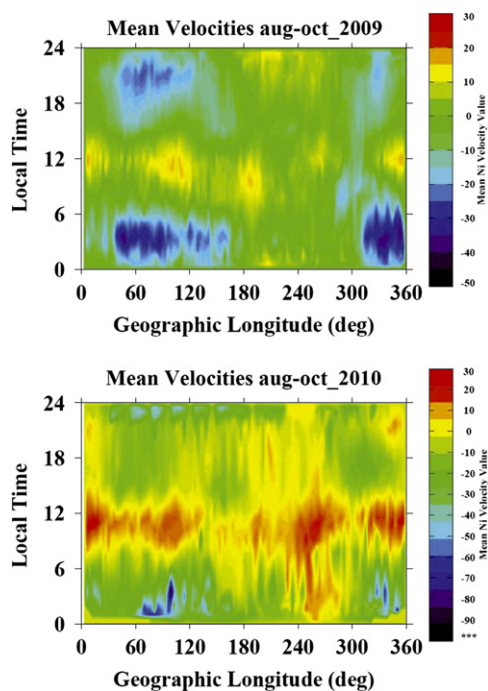


Fig. 3. Mean meridional velocities from IVM are shown for two 3-month periods during 2009 (top) and 2010 (bottom).

between 200° and 360° . At post-sunset local times, there is a maximum around 270° – 290° , followed by a minimum at 320° – 330° . At 3.25 LT these are reversed, with a deep minimum observed around 260° – 290° , followed by a maximum at 320° – 330° . This behavior is consistent for all three northern summer solstices.

An analysis of the neutral densities derived from the GRACE accelerometers has been carried out, and those results reported by Huang et al. (2011). The salient points are repeated here for clarity. In Fig. 6 the C/NOFS PLP dayside plasma and GRACE

neutral density residuals for the 10–12 LT sector during June 2008 are shown. Note that the error bars in Fig. 6 which show the standard deviations for each data point plotted are representative of the two datasets in general. There is no direct correlation between the plasma and neutrals, as expected (Immel et al., 2006). The correlation coefficient calculated for the two sets of data shown in Fig. 6 is 0.13. Tidal features are apparent in the plasma densities, but not in the neutrals, on the dayside. As can be seen in Fig. 2, the 4-wave structure in plasma densities is not apparent on the nightside.

On the nightside, the neutrals show wavenumber-4 periodicity, as shown in Fig. 7. GRACE neutral density residuals are shown for the 20–22 LT sector during June 2008. Also shown in Fig. 7 is the zonal drift measured by VEFI for the same period and 21.75 LT. There is an apparent correlation between the two sets of data which were obtained from different instruments on different spacecraft, widely separated in orbital altitude and inclination. The correlation coefficient between the two sets of data plotted in Fig. 7 is 0.71. While this number is not proof that the two parameters are causally related, it does suggest a connection.

In both sets of data shown in Fig. 7, the minimum in this local time sector is reached at about 330° , the same location as the minimum in plasma density in BPDs. As we have already reported (Huang et al., 2012), the ion and neutral density minima occur where meridional velocity is also a minimum, reaching -45 m/s as shown in Fig. 3. There are no observations of vertical winds during these periods so we cannot compare the relative speeds of ions to neutrals, but it seems unlikely that vertical winds in excess of -45 m/s are common.

Large plasma depletions have been reported in other C/NOFS studies (Su et al., 2009, 2011; Burke et al., 2009; de La Beaujardière et al., 2009) as well as in DMSP papers (Gentile et al., 2011). Their cause has aroused much speculation. As we pointed out (Huang et al., 2009, 2011) the BPD occurs in the minimum of the tidal pattern between 300° and 360° . This is a persistent and repeatable feature of the equatorial ionosphere during solar minima, at all altitudes from 400–840 km. In Fig. 8 are shown the total numbers of dawn depletions observed by

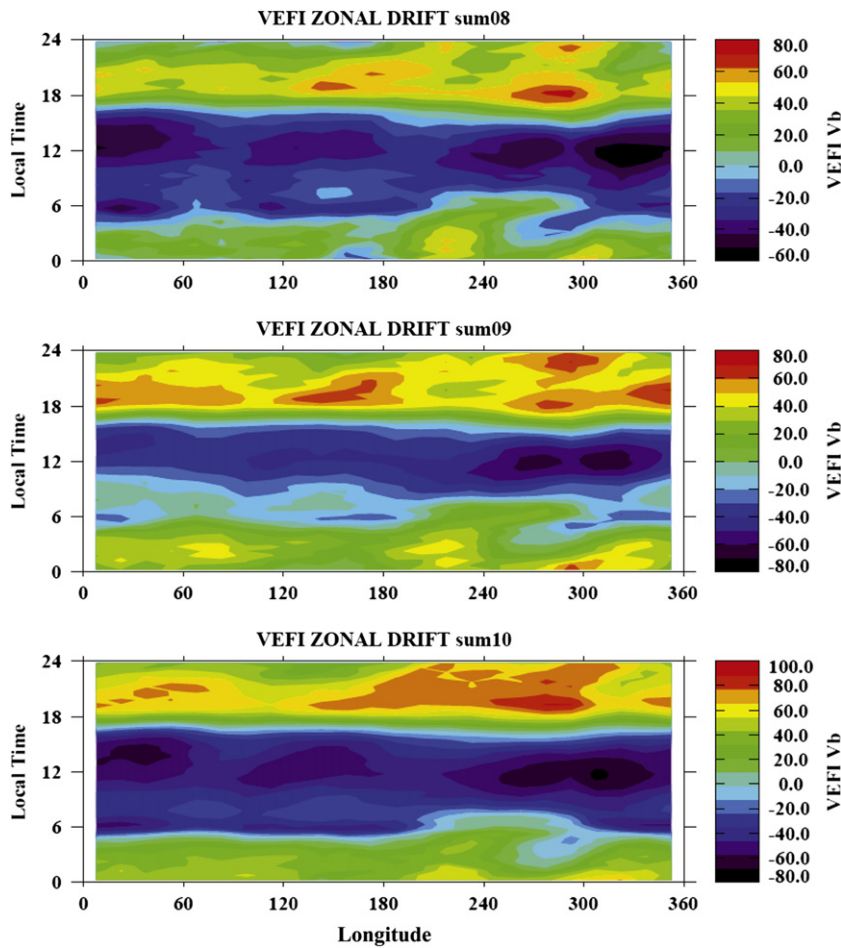


Fig. 4. VEFI zonal drifts averaged over 120 days are shown during northern summer solstices in 2008 (top), 2009 (middle) and 2010 (bottom).

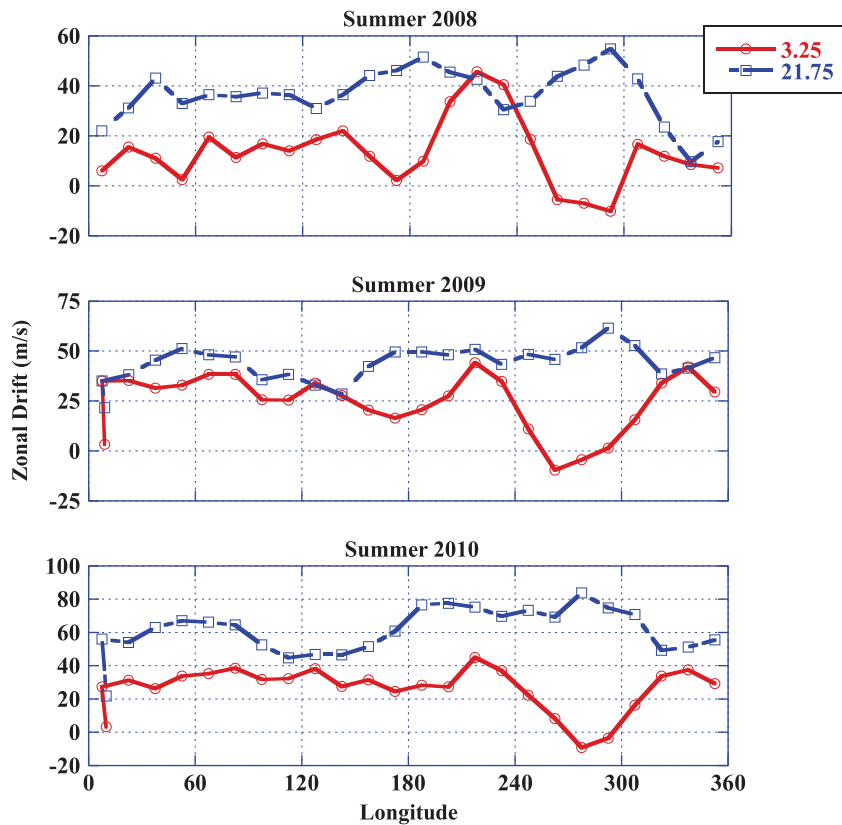


Fig. 5. VEFI zonal drifts for two local times on the nightside are shown for the same three summer solstice periods as in Fig. 4. The post-sunset LT (blue) and post-midnight LT (red) are plotted. (For interpretation of the references to color in this figure legend, the reader is referred to the web version of this article.)

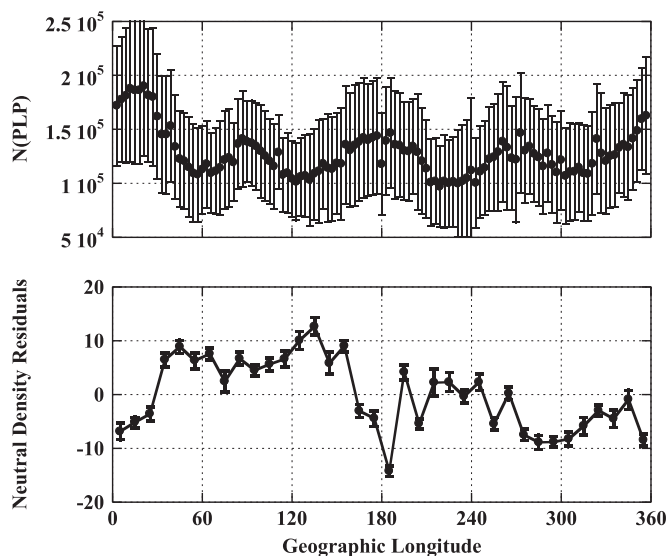


Fig. 6. Detrended PLP densities with standard deviations for 10–12 LT during June 2008 are shown (top), together with neutral density residuals from GRACE (bottom) during the same time interval, local time and latitudinal coverage as C/NOFS.

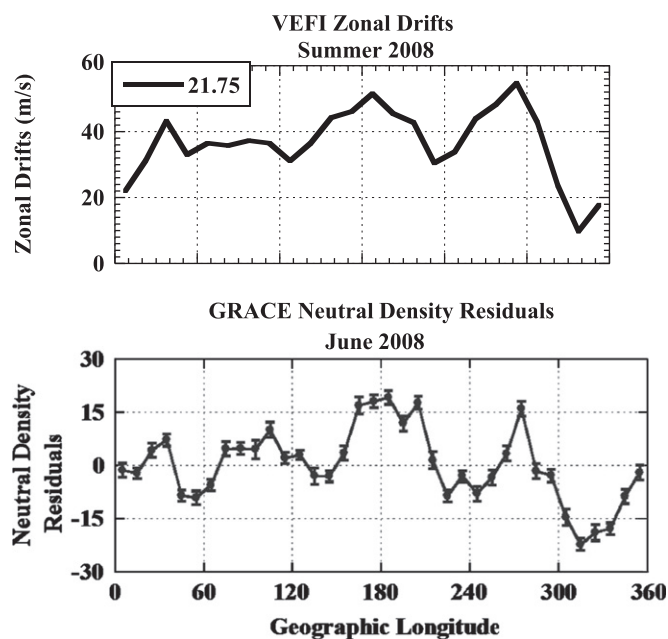


Fig. 7. VEFI zonal drift at 21.75 LT is shown during the summer solstice of 2008 (top), together with the GRACE neutral density residuals for 20–22 LT for the same period.

DMSP F17 during the years 2008–2010 (adapted from Gentile et al., 2011). There was a sharp upturn in occurrence from 2007 to 2008 which persisted in 2009. The overall shape of the plot follows the pattern of wavenumber-4 tidal signatures reported by C/NOFS investigations, where the maximum numbers of events coincide with minima in the tidal pattern. Further, the highest occurrence of dawn depletions is around 310° longitude coincident with BPD locations. These dawn depletions occur predominantly during June of each year, with a secondary maximum at about 60° which occurs during December.

In Fig. 9 the dawn depletions observed on DMSP F17 during 2009 (top), with the C/NOFS IVM meridional velocity at 0530 LT for the three-month period centered on June 2009 (bottom) are shown. Both sets of data are measured close to the dawn local

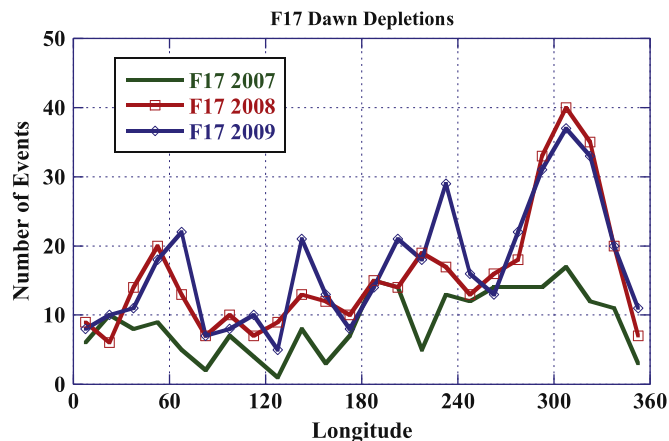


Fig. 8. Occurrences of dawn depletions from the DMSP F17 satellite are shown for three years, 2007 (green), 2008 (red) and 2009 (blue) (adapted from Gentile et al., 2011). (For interpretation of the references to color in this figure legend, the reader is referred to the web version of this article.)

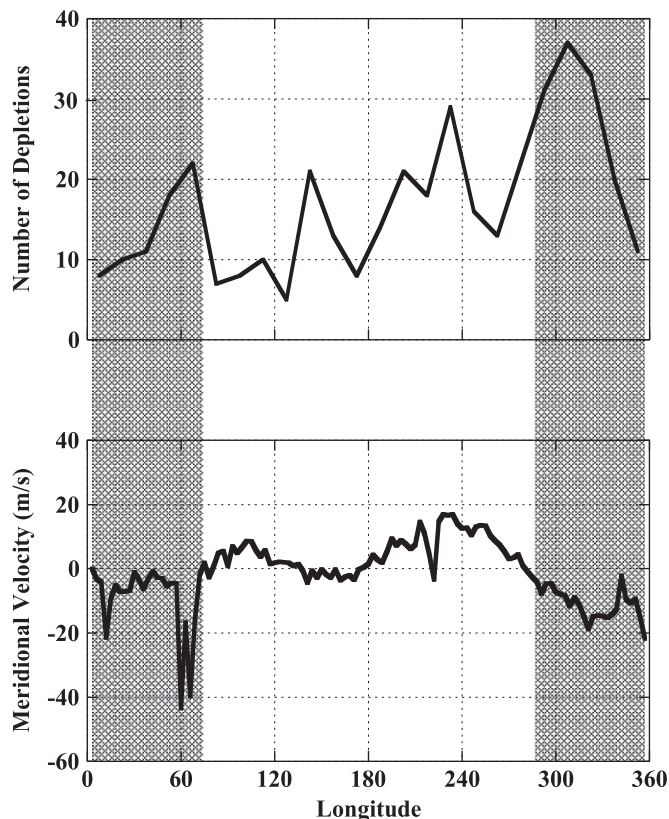


Fig. 9. DMSP F17 dawn depletions during 2009 are shown at top, IVM meridional velocity at 0530 LT during the 3-month interval centered on June 2009 is shown below. Shaded areas denote longitudinal ranges where meridional velocity is negative, or directed downward.

time sector. The two plots are roughly anti-correlated, most strikingly around 300° longitude. Regions of depleted plasma coincide most frequently with downward meridional velocity, indicated by shading. This is also true around 60° where velocity is sharply negative, but the remaining two maxima in the number of depletions coincide with zero or slightly upward velocity. As pointed out earlier, the IVM meridional velocity reaches its maximum downward value between 300° and 360° , the prime location for BPD occurrence. This maximum is attained at 20–22 LT as can be seen in Fig. 3.

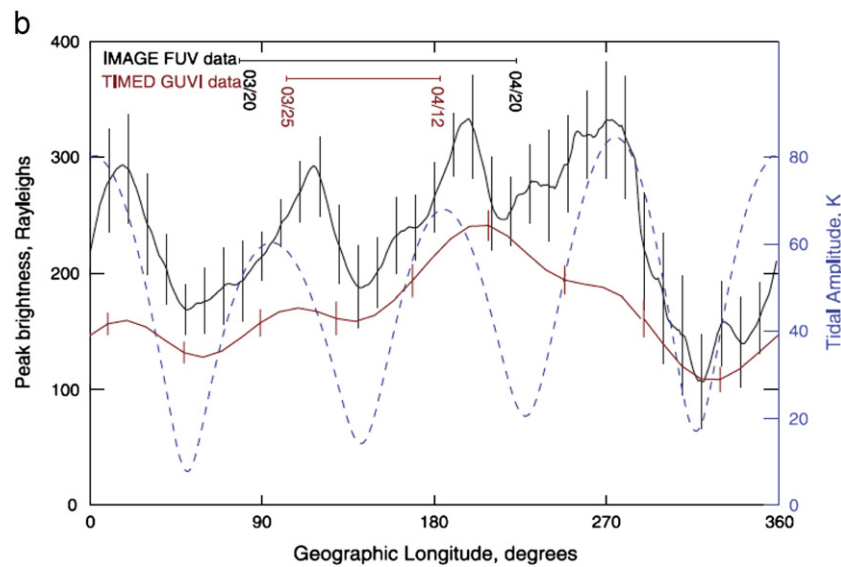


Fig. 10. FUV data from IMAGE (solid black line) and GUVI data from TIMED (solid red line) missions (edited from Fig. 4 of *Immel et al., 2006*), together with results of the TIME-GCM model (dashed blue line). (For interpretation of the references to color in this figure legend, the reader is referred to the web version of this article.)

There are other incidences of plasma depletions which bear a remarkable resemblance to BPDs or dawn depletions. In *Fig. 10* we show a figure from *Immel et al. (2006)* (edited from their *Fig. 4*) in which brightness from the IMAGE FUV and TIMED GUVI instruments is plotted as functions of longitude. The 4-wave structure can be readily seen in both sets of observations. A large drop in brightness, and hence plasma density, can be observed peaking at about 315° , the same location as BPDs and dawn depletions. These observations were made during solar maximum over the equatorial anomalies, so there is a difference between these results and the ones in this paper.

4. Discussion

The data obtained by three independent instruments on the C/NOFS satellite all display wavenumber-4 periodicity during the 2008–2010 interval. The PLP, IVM and VEFI measure plasma density, meridional and zonal velocities, all of which are strongly influenced by tidal forces. Note that the plasma data presented in *Figs. 1 and 2* are absolute densities, not residuals or the results of processing to extract wave components. The tidal signatures are strongest in June–September, and weakest in December. This climatology, which is repeated during 2008–2010, is similar to that of DE-3 nonmigrating tides (*Hagan and Forbes, 2002, 2003*) as predicted by the Global Scale Wave Model (*Hagan et al., 2001*).

There are distinctions between the three sets of data in this study. PLP and IVM show waves which are strong on the dayside, but weak to nonexistent on the nightside. VEFI data show weak waves present on the nightside, with phase shifts between local time sectors. In post-midnight LT sectors, a distinctive pattern emerges with maxima at 210° and 330° and minima at 270° and 360° . This effect is seen clearly during June solstice months from 2008 to 2010. This pattern is not correlated with the zonal drifts observed just after sunset.

In all three instruments, the strongest waves are detected during the June solstices, a difference between the C/NOFS results and the standard climatology for DE3 tidal modes. It is possible that the extremely low values of F10.7 affected the effective penetration of tidal forcing. It should be noted that we have not carried out an analysis of the modes present in the observations reported in this paper. It is highly probable that modes other than

DE3 are present which can give rise to wavenumber-4 features as well as contribute constructively or destructively to the appearance of the tidal structures. Our analysis of the neutral density residuals from the GRACE accelerometer data revealed the presence of SE2 modes during certain seasons, although DE-3 was dominant during northern summer months. Similar analysis has been carried out by *Oberheide et al. (2011)*, *Pancheva et al. (2012)* and others which show the presence of other modes such as SPW4 and SE2 which contribute to, and modulate the wavenumber-4 structures.

Our analysis of neutral densities from the GRACE accelerometer shows the presence of tides during June 2008, but DE3 is only clearly detected on the nightside. An analysis of the different tidal modes present during this period shows a number of modes which interfere destructively on the dayside, but on the nightside the strongest feature is the DE3 nonmigrating tide. This distinguishes the neutral tides from our ion density analysis during this interval.

There is an intriguing correlation between VEFI zonal drifts and GRACE neutral density residuals at 20–22 LT. It suggests that the zonal drifts correlate with zonal winds which are related to the neutral tidal structures (*Hausler et al., 2007*). The correlation coefficient of 71% suggests that zonal drifts may be used as a proxy for neutral winds when direct wind measurements are absent. We intend to follow this up with further analysis.

The BPDs which were detected initially using PLP appear to be a part of the tidal structure, but the nature of the ion-neutral coupling which forms the large depletions is still unknown. From the average meridional velocities measured by IVM and shown in *Fig. 3*, they are formed in regions of downward-directed plasma velocity. Dawn depletions from DMSP exhibit large plasma decreases with similar climatology to BPDs in that the largest depletions are detected between 300° and 360° , and the highest frequency of occurrence happens during June solstices in 2007–2009. When the DMSP dawn depletions during 2009 are compared with the IVM meridional velocity at 6 UT for June 2009, it is apparent that the large depletions around 330° coincide with downward-directed plasma velocity.

The neutral density residuals also exhibit large decreases in the same longitudinal and local time sectors as the BPDs. These locations are also where the meridional velocity is large and downward, and about 60° in longitude east of the minimum in

nightside zonal drift. These observations suggest that some form of ion-neutral coupling accounts for the large decreases in both ion and neutral densities. In the absence of neutral wind measurements, we can only speculate that the large downward meridional velocity of up to -45 m/s suggests that ion drag is responsible for the neutral density depletions. This would be very surprising, given the relative momentum carried by ion and neutrals, but we are not aware of vertical drifts much larger than 45 m/s which would be necessary if neutral winds were the driver.

From the C/NOFS PLP averages reported earlier (Huang et al., 2011) BPDs on the dayside and particularly across the entire nightside coincide with the largest and most frequent DMSP dawn depletions around 330° . We suggest that these large depletions are a persistent feature of the tidal pattern and are not restricted only to dawn local times. This was confirmed by Huang et al. (2009) in which BPDs on DMSP at around 20 LT were reported as a regular occurrence during solar minimum. Further evidence that BPDs are a regular occurrence comes from the IMAGE and GUVI UV images shown in Fig. 10. It should be noted that these images were obtained during solar maximum and on the nightside (20 LT for the interval from 20 March–20 April 2002), but show the same large decrease in plasma density in the same geographic location as BPDs.

There have been some efforts to explain BPDs. Hagan et al. (2007) modeled the equatorial region with the Thermosphere–Ionosphere–Mesosphere–Electrodynamics General Circulation Model (TIME-GCM), taking into account the offset between the geographic equator and the IGRF magnetic equator. The effect of forcing from the troposphere is also included. This produced a 4-wave periodic structure with longitudinal variations which peak where the offset is greatest, around 300° longitude. This is not the longitude where the BPDs maximize which is closer to 330° , and the predicted variation in plasma density is not as large as the observations indicate, but this effect may be a partial solution to the mystery of BPD formation.

5. Summary

We have presented observations made with the PLP, IVM and VEFI instruments on C/NOFS. Detrended PLP densities, meridional ion velocity data from IVM, and zonal drifts from VEFI all exhibit tidal wave patterns during the 2 years following the launch of C/NOFS in 2008. There are similarities in all three datasets, but also differences. All three show strong wavenumber-4 periodicity on the dayside between June–September, in agreement with the climatology of the DE-3 tidal mode. However the C/NOFS tidal structures are strongest during June and not September, as expected for DE3 waves.

Zonal drifts from VEFI show 4-wave structure on the nightside, a difference between VEFI and the PLP or IVM results. The nightside waves in VEFI zonal drifts evolve from early to late local times, with a phase change most noticeable from about 180° to 360° longitude.

Tidal structures were also detected by the GRACE accelerometers during the same time intervals. A comparison of the neutral density residuals from GRACE and the average plasma density during June 2008 reveals that there is little similarity between neutral and plasma tides. The PLP data show tidal features most strongly on the dayside, while the GRACE data show clear wave structures only on the nightside. However there is one recurring similarity. Both ion and neutral densities display a deep and broad decrease between 300° and 360° longitude, with a minimum at about 330° . This feature has been described as a Broad Plasma Decrease in past papers (Huang et al., 2009, 2011, 2012).

A comparison of C/NOFS zonal drifts and GRACE neutral density residuals during June 2008, at 20–22 LT, shows a correlation coefficient of 71%. The similarity in the two sets of data is surprising, given that they are different physical parameters being measured by different instruments on widely separated spacecraft. We speculate that the zonal drifts may be closely related to zonal winds which are associated with neutral density tidal structures (Hausler et al., 2007). If this speculation is borne out by further investigation, it may be a way to obtain zonal winds in a region where there are scant measurements.

Dawn depletions, which have been reported on C/NOFS as well as DMSP show an anti-correlation with C/NOFS meridional velocity. The higher occurrence frequencies of dawn depletions are correlated with downward-directed meridional velocity. Both phenomena occur in the same longitudinal sector as BPDs. Further, the DMSP dawn depletions show the same tidal signature as has been reported in several C/NOFS-based studies (Araujo-Pradere et al., 2012; Dao et al., 2011). We suggest that these depletions have the same physical basis as BPDs, and that both are features of the 4-wave tidal periodicity which dominates the ionosphere during solar minimum. In other studies of large depletions using DMSP, they have been detected in the evening sector indicating that they are not restricted to dawn locations (Huang et al., 2009). One consistent result is that the DMSP depletions and the BPDs are most prominent in the 300° – 360° longitudinal region, which is also where the meridional and zonal velocities reach minima.

Large plasma decreases have been reported by other investigators. The UV imagers on IMAGE and TIMED detected peak radiances with wavenumber-4 tidal periodicity during the 20 March–20 April interval in 2002 (Immel et al., 2006). The tidal pattern overlaid a large decrease in radiance around 330° . This decrease in radiance corresponds to a decrease in plasma density. It should be noted that these observations were made during solar maximum, while all the other observations in our paper are for solar minimum conditions.

A modeling effort by Hagan et al. (2007) in which tropospheric forcing and the offset of the magnetic dipole equator from the geographic equator were included, succeeded in producing a tidal pattern in plasma density with longitudinal variation peaking at about 300° . Detailed results do not reproduce the BPDs which peak closer to 330° , and the variation in observed plasma density exceeds the model prediction, but it indicates that these physical factors must be considered in order to predict ionospheric structure in the equatorial region. A fuller and more accurate explanation of BPD formation has yet to be put forward.

Acknowledgments

The C/NOFS mission is supported by the Air Force Research Laboratory, the Department of Defense Space Test Program, the National Aeronautics and Space Administration, the Naval Research Laboratory, and the Aerospace Corporation. This research was supported by Air Force Office of Scientific Research Task 12RV120COR. We thank Dr. John Retterer for his assistance with VEFI data processing.

References

- Araujo-Pradere, E.A., Fang, T.-W., Anderson, D.N., Fedrizzi, M., Stoneback, R., 2012. Modeling the daytime, equatorial ionospheric ion densities associated with the observed, four-cell longitude patterns in $E \times B$ drift velocities. *Radio Science* 47, RS0L12, <http://dx.doi.org/10.1029/2011RS004930>.
- Bilitza, D., Reinisch, B., 2008. International reference ionosphere 2007: improvements and new parameters. *Advances in Space Research* 42 (4), 599–609, <http://dx.doi.org/10.1016/j.asr.2007.07.048>.

- Bruinsma, S., Tamagnan, D., Biancale, R., 2004. Atmospheric densities derived from CHAMP/STAR accelerometer observations. *Planetary and Space Science* 52, 297.
- Burke, W.J., de La Beaujardière, O., Gentile, L.C., Hunton, D.E., Pfaff, R.F., Roddy, P.A., Su, Y.-J., Wilson, G.R., 2009. C/NOFS observations of plasma density and electric field irregularities at post-midnight local times. *Geophysical Research Letters* 36, L00C09, <http://dx.doi.org/10.1029/2009GL038879>.
- Dao, E.V., Kelley, M.C., Roddy, P., Retterer, J., Ballenthin, J.O., de La Beaujardière, O., Su, Y.-J., 2011. Longitudinal and seasonal dependence of nighttime equatorial plasma density irregularities during solar minimum detected on the C/NOFS satellite. *Geophysical Research Letters* 38, L10104, <http://dx.doi.org/10.1029/2011GL047046>.
- de La Beaujardière, O., Jeong, L., Basu, B., Basu, S., Beach, T., Bernhardt, P., Burke, W., Groves, K., Heelis, R., Holzworth, R., Huang, C., Hunton, D., Kelley, M., Pfaff, R., Retterer, J., Rich, F., Starks, M., Straus, P., Valladares, C., 2004. C/NOFS: a mission to forecast scintillations. *Journal of Atmospheric and Solar-Terrestrial Physics* 66, 1573.
- de La Beaujardière, O., Retterer, J.M., Pfaff, R.F., Roddy, P.A., Roth, C., Burke, W.J., Su, Y.-J., Kelley, M.C., Ilma, R.R., Wilson, G.R., Gentile, L.C., Hunton, D.E., Cooke, D.L., 2009. C/NOFS observations of deep plasma depletions at dawn. *Geophysical Research Letters* 36, L00C06, <http://dx.doi.org/10.1029/2009GL038884>.
- Gentile, L.C., Burke, W.J., Roddy, P.A., Retterer, J.M., Tsunoda, R.T., 2011. Climatology of plasma density depletions observed by DMSP in the dawn sector. *Journal of Geophysical Research* 116, A03321, <http://dx.doi.org/10.1029/2010JA016176>.
- Hagan, M.E., Forbes, J.M., 2002. Migrating and nonmigrating diurnal tides in the middle and upper atmosphere excited by tropospheric latent heat release. *Journal of Geophysical Research* 107 (D24), 4754, <http://dx.doi.org/10.1029/2001JD001236>.
- Hagan, M.E., Forbes, J.M., 2003. Migrating and nonmigrating semi-diurnal tides in the middle and upper atmosphere excited by tropospheric latent heat release. *Journal of Geophysical Research* 108 (A2), 1062, <http://dx.doi.org/10.1029/2002JA009466>.
- Hagan, M.E., Maute, A., Roble, R.G., Richmond, A.D., Immel, T.J., England, S.L., 2007. Connections between deep tropical clouds and the Earth's ionosphere. *Geophysical Research Letters* 34, L20109, <http://dx.doi.org/10.1029/2007GL030142>.
- Hagan, M.E., Roble, R.G., Hackney, J., 2001. Migrating thermospheric tides. *Journal of Geophysical Research* 106, 12739–12752.
- Hausler, K., Luhr, H., Rentz, S., Kohler, W., 2007. A statistical analysis of longitudinal dependences of upper thermospheric zonal winds at dip equator latitudes derived from CHAMP. *Journal of Atmospheric and Solar-Terrestrial Physics* 69, 1419–1430, <http://dx.doi.org/10.1016/j.jastp.2007.04.004>.
- Heelis, R.A., Coley, W.R., Burrell, A.G., Hairston, M.R., Earle, G.D., Perdue, M.D., Power, R.A., Harmon, L.L., Holt, B.J., Lippincott, C.R., 2009. Behavior of the O⁺/H⁺ transition height during the extreme solar minimum of 2008. *Geophysical Research Letters* 36, L00C03, <http://dx.doi.org/10.1029/2009GL038652>.
- Huang, C.S., Rich, F.J., de La Beaujardière, O., Heelis, R.A., 2010. Longitudinal and seasonal variations of the equatorial ionospheric ion density and eastward drift velocity in the dusk sector. *Journal of Geophysical Research* 115, A02305, <http://dx.doi.org/10.1029/2009JA014503>.
- Huang, C.Y., Marcos, F.A., Roddy, P.A., Hairston, M.R., Coley, W.R., Roth, C., Bruinsma, S., Hunton, D.E., 2009. Broad plasma decreases in the equatorial ionosphere. *Geophysical Research Letters* 36, L00C04, <http://dx.doi.org/10.1029/2009GL039423>.
- Huang, C.Y., Delay, S.H., Roddy, P.A., Sutton, E.K., 2011. Periodic structures in the equatorial ionosphere. *Radio Science* 46, RD0D14, <http://dx.doi.org/10.1029/2010RS004569>.
- Huang, C.Y., Delay, S.H., Roddy, P.A., Sutton, E.K., Stoneback, R. Longitudinal structures in the equatorial ionosphere during deep solar minimum. *Journal of Atmospheric and Solar-Terrestrial Physics*, in press.
- Immel, T.J., Sagawa, E., England, S.L., Henderson, S.B., Hagan, M.E., Mende, S.B., Frey, H.U., Swenson, C.M., Paxton, L.J., 2006. Control of equatorial ionospheric morphology by atmospheric tides. *Geophysical Research Letters* 33, L15108, <http://dx.doi.org/10.1029/2006GL026161>.
- Kil, H., Oh, S.-J., Kelley, M.C., Paxton, L.J., England, S.L., Talaat, E., Min, K.-W., Su, S.-Y., 2007. Longitudinal structure of the vertical E × B drift and ion density seen from ROCSAT-1. *Geophysical Research Letters* 34, L14110, <http://dx.doi.org/10.1029/2007GL030018>.
- Lin, C.H., Hsiao, C.C., Liu, J.Y., Liu, C.H., 2007. Longitudinal structure of the equatorial ionosphere: time evolution of the four-peaked EIA structure. *Journal of Geophysical Research* 112, A12305, <http://dx.doi.org/10.1029/2007JA012455>.
- Lindzen, R.S., Chapman, S., 1969. Atmospheric tides. *Space Science Reviews* 10, 3.
- Liu, H., Watanabe, S., 2008. Seasonal variation of the longitudinal structure of the equatorial ionosphere: does it reflect tidal influences from below. *Journal of Geophysical Research* 113, A083115, <http://dx.doi.org/10.1029/2008JA013017>.
- Luhr, H., Hausler, K., Stolle, C., 2007. Longitudinal variation of F region electron density and thermospheric zonal wind caused by atmospheric tides. *Geophysical Research Letters* 34, L16102, <http://dx.doi.org/10.1029/2007GL030639>.
- Maynard, N.C., 1998. Electric field measurements in moderate to high density space plasmas with passive double probes. In: Pfaff, R.F., Borovsky, J.E., Young, D.T. (Eds.), *Measurement Techniques in Space Plasmas: Fields*. American Geophysical Union, Washington D.C. pp. 13–27.
- Oberheide, J., Forbes, J.M., Zhang, X., Bruinsma, S.L., 2011. Wave-driven variability in the ionosphere thermosphere-mesosphere system from TIMED observations: What contributes to the “wave 4”? *Journal of Geophysical Research* 116, A01306, <http://dx.doi.org/10.1029/2010JA015911>.
- Pancheva, D., Miyoshi, Y., Mukhtarov, P., Jin, H., Shinagawa, H., Fujiwara, H., 2012. Global response of the ionosphere to atmospheric tides forced from below: comparison between COSMIC measurements and simulations by atmosphere-ionosphere coupled model GAIA. *Journal of Geophysical Research* 117, A07319, <http://dx.doi.org/10.1029/2011JA017452>.
- Pancheva, D., Mukhtarov, P., 2010. Strong evidence for the tidal control on the longitudinal structure of the ionospheric F region. *Geophysical Research Letters* 35, L14105, <http://dx.doi.org/10.1029/2010GL044039>.
- Pedatella, N.M., Forbes, J.M., Oberheide, J., 2008. Intra-annual variability of the low-latitude ionosphere due to nonmigrating tides. *Geophysical Research Letters* 35, L18104, <http://dx.doi.org/10.1029/2008GL035332>.
- Pfaff, R.F., Freudenreich, H., Klenzing, J.H., Rowland, D.E., Liebrecht, M.C., Bromund, K.R., Roddy, P.A., 2010a. Persistent longitudinal variations of plasma density and DC electric fields in the low latitude ionosphere observed with probes on the C/NOFS satellite, SA 41C-03. In: *Proceedings of Fall AGU meeting*.
- Pfaff, R.F., Rowland, D., Freudenreich, H., Bromund, K., Le, G., Acuña, M., Klenzing, J., Liebrecht, C., Martin, S., Burke, W.J., Maynard, N.C., Hunton, D.E., Roddy, P.A., Ballenthin, J.O., Wilson, G.R., 2010b. Observations of DC electric fields in the low-latitude ionosphere and their variations with local time, longitude, and plasma density during extreme solar minimum. *Journal of Geophysical Research* 115, A12324, <http://dx.doi.org/10.1029/2010JA016023>.
- Ren, Z., Wang, W., Liu, L., Zhao, B., Wei, Y., Yue, X., Heelis, R.A., 2008. Longitudinal variations of electron temperature and total ion density in the sunset equatorial topside ionosphere. *Geophysical Research Letters* 35, L05108, <http://dx.doi.org/10.1029/2007GL032998>.
- Rich, F.J., Hairston, M., 1994. Large-scale convection patterns observed by DMSP. *Journal of Geophysical Research* 99 (A3), 3827–3844, <http://dx.doi.org/10.1029/93JA03296>.
- Scherliess, L., Thompson, D.C., Schunk, R.W., 2008. Longitudinal variability of low-latitude total electron content: tidal influences. *Journal of Geophysical Research* 113, A01311, <http://dx.doi.org/10.1029/2007JA012480>.
- Su, Y.-J., Retterer, J.M., de La Beaujardière, O., Burke, W.J., Roddy, P.A., Pfaff Jr., R.F., Wilson, G.R., Hunton, D.E., 2009. Assimilative modeling of equatorial plasma depletions observed by C/NOFS. *Geophysical Research Letters* 36, L00C02, <http://dx.doi.org/10.1029/2009GL038946>.
- Su, Y.J., Retterer, J.M., Pfaff, R.F., Roddy, P.A., de La Beaujardière, O., Ballenthin, J.O., 2011. Assimilative modeling of observed postmidnight equatorial plasma depletions in June 2008. *Journal of Geophysical Research* 116, A09318, <http://dx.doi.org/10.1029/2011JA016772>.
- Sutton, E.K., 2009. Normalized force coefficients on for satellites with elongated shapes. *Journal of Spacecraft and Rockets* 46 (1), 112–116, <http://dx.doi.org/10.2514/1.40940>.
- Sutton, E.K., Forbes, J.M., Nerem, R.S., 2005. Global thermospheric neutral density and wind response to the severe 2003 geomagnetic storms from CHAMP accelerometer data. *Journal of Geophysical Research* 110, A09S40, <http://dx.doi.org/10.1029/2004JA010985>.